IEEE Access
Multidisciplinary | Rapid Review | Open Access Journal

Received November 16, 2017, accepted December 15, 2017, date of publication January 5, 2018, date of current version February 28, 2018.

Digital Object Identifier 10.1109/ACCESS.2018.2790038

RF Energy Absorption by Biological Tissues in Close Proximity to Millimeter-Wave 5G Wireless Equipment

DAVIDE COLOMBI[1], BJÖRN THORS[1], CHRISTER TÖRNEVIK[1], (Member, IEEE), AND QUIRINO BALZANO[2]

[1]Ericsson Research, Ericsson AB, Stockholm SE-16480, Sweden
[2]Department of Electrical and Computer Engineering, University of Maryland, College Park, MD 20742 USA

Corresponding author: Davide Colombi (davide.colombi@ericsson.com)

ABSTRACT In this paper, mechanisms of RF energy absorption by body tissue in close proximity to wireless equipment, are studied using numerical simulations at frequencies above 24 GHz. It is shown that at millimeter-wave (mmW) frequencies, of relevance for 5G mobile communications, and for realistic source to body separation distances, the contribution from the reactive near-field to the energy deposition in the tissue is small. Furthermore, the interaction between the source and the exposed body is modest. The results suggest that the effects of the near-field body interactions are small when evaluating electromagnetic field compliance at mmW frequencies.

INDEX TERMS Human exposure, energy absorption, millimeter waves, 5G mobile communication, mobile devices.

I. INTRODUCTION

During the last decades, large research efforts have been spent to characterize exposure to radiofrequency (RF) electromagnetic field (EMF) below 10 GHz, i.e. for those bands where the vast majority of current radio communication sources operate. International exposure limits such as those recommended by the International Commission on Non-Ionizing Radiation Protection (ICNIRP, [1]) as well as EMF compliance testing methodologies and procedures (e.g. [2]) in this frequency range have been defined based on extensive available knowledge. For higher frequency bands, the amount of research results is more limited, exposure restrictions less detailed and test methodologies less mature due to fewer technologies using this spectrum. Frequency bands within the centimeter and millimeter wave range, however, are key components of the next generation mobile network, 5G [3], which is expected to be commercially available before 2020.

The ICNIRP RF EMF exposure limits have been developed to protect, with wide safety margins, from established adverse health effects related to heating of body tissue [1]. The development of thermal models useful to predict the skin temperature increase due to exposure in the millimeter wave frequency range has been the subject of some recent studies [4]–[7]. Some authors provided insights on exposure assessment methodologies in this frequency range [8]–[10] or have investigated the implications that the current EMF exposure limits may have on future wireless devices [11]–[13].

On the other hand, the vast majority of literature studying the near-field interaction between biological bodies and antennas has focused on frequencies below 3 GHz (e.g. [14]). Some aspects at higher frequencies were investigated numerically and experimentally in [15] but were limited to body-area network applications, for a unique antenna operating at 60 GHz explicitly designed to minimize the influence of the body on the radiation performance. Modelling of the millimeter wave interaction with the skin was conducted in [16] but was only based on plane-wave far-field exposure at normal incidence to the skin surface.

At 10 GHz the fundamental exposure metric defined by ICNIRP changes from specific absorption rate (SAR) to incident power density. Analogous transitions are specified by other regulatory authorities and standardization bodies (such as the Federal Communications Commission and IEEE). As the frequency is increased the depth of penetration of RF fields becomes smaller. SAR limits, intended as averaged over the entire body mass or over 10 g of body tissue are not relevant when energy deposition occurs only close to the skin surface. In addition, the field strength in a thin superficial volume becomes cumbersome to measure. For these reasons, the relevant exposure parameter specified by the guidelines is incident power density at the higher frequencies.

The power density limits above 10 GHz were developed mainly assuming far-field conditions, due to the lack of devices intended to be used near the body in this band. The suitability of these limits for mobile phones, tablets or other devices operated near the body therefore needs to be investigated. Because power density is measured in free-space, without the presence of the body or a body model, it is of interest to quantify the impact on energy absorption from coupling between the antenna and the exposed body at frequencies above 10 GHz.

In this work, energy absorption mechanisms including effects of body-antenna interactions were analyzed at frequencies above 10 GHz in the near-field of realistic sources. This investigation provides useful insights for the development of relevant exposure limits applicable to the next generation of wireless equipment and of procedures for EMF compliance testing of products operating in these bands.

II. METHODS

Several factors contribute to the RF energy deposition from sources positioned in close proximity to the human body:

- Part of the reactive near field energy around the antenna is coupled and absorbed.
- The wave incident on the body is partly absorbed and partly reflected by the tissue. Some of the reflected energy might also couple to the source and be partly re-transmitted. This process may be repeated iteratively and the absorbed power may therefore be characterized in terms of a sum of multiple antenna-body interactions [17].
- The presence of multiple interactions might influence the actual current distribution on the antenna and the absorbed energy profile.
- Part of the reflected energy might couple through the antenna port to the generator load, changing the input impedance and the antenna matching.

This implies that in the near field the coupling of the antenna with the body may have a substantial impact on the transfer of energy from the source to the tissues. When increasing the frequency (reducing the wavelength) this effect is expected to decrease. Its relevance in (or around) the millimeter wave range was evaluated by means of numerical modelling of different sources. The frequencies targeted were those of main interest for 5G, i.e. primary above 24 GHz [18].

Antenna models were chosen to be representative for a wide class of portable devices including both directional and omni-directional transmitters. In these higher frequency bands, user equipment will make use of MIMO and beamforming to optimize transmission (e.g. [19]). For this reason, an array of four dipoles and a slot array with 4 ports were selected in addition to two single element antennas, a canonical dipole and a Planar Inverted-F Antenna (PIFA). Antenna dimensions are provided in Fig. 1 and were scaled with the operating frequency. All metallic parts were modelled as perfect electric conductors. The blue-red dots in Fig.1 represent the antenna ports; the elements were excited with voltage sources of equal amplitude and phase. The notch array is characterized by four ports with notches cut on the top. Parasitic notches are cut between adjacent radiating notches to reduce mutual coupling [9].

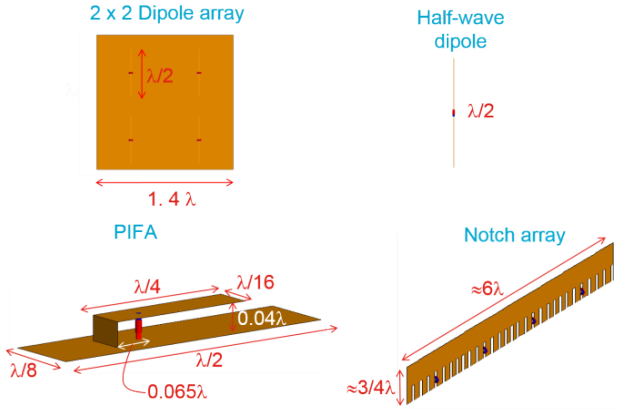

FIGURE 1. Antenna geometries. λ is the wavelength in free-space; the blue-red dots represent the antenna ports.

Numerical simulations were conducted using the commercial electromagnetic solver FEKO (Altair, Stellenbosch, South Africa) based on the Method of Moments. Antennas were meshed using triangles with a maximum edge length of λ/16. The dipoles were modeled as thin wires with a maximum segment length of λ/16.

The exposed body was modelled as a homogenous half-space with dielectric properties equal to the average between wet and dry skin as reported by Gabriel *et al.* [20]. In [16] it was shown that, due to the shallow field penetration, a homogenous skin model is suitable to accurately describe the absorbed energy profile in the millimeter wave frequency range for tissues characterized by thin stratum corneum. The dielectric values for the frequencies investigated in this paper are reported in Table 1.

TABLE 1. Dielectric properties of the skin (averaged between dry and wet) as used in the model.

	24GHz	30 GHz	45 GHz	60 GHz
ε_r	20.0	16.6	11.6	9.1
σ (S/m)	23.0	27.3	34.2	38.0

The simulations were conducted with the antennas oriented to make their main beams point perpendicularly to the tissue half-space. This configuration was selected since it is expected to maximize the antenna-tissue coupling.

In Section III results are presented for several separation distances (ranging from 5 mm to 50 mm) from the tissue model surface to the closest point of the antenna.

A. EFFECT OF THE REACTIVE NEAR-FIELD

The energy per unit time crossing the infinitesimal surface dA, or the energy flux rate, is determined through assessment of the Poynting vector and is defined as

$$P_{\mathrm{dA}} = \frac{1}{2}\Re\left(\mathbf{E}\times\mathbf{H}^{*}\right)\cdot\mathbf{dA}, \tag{1}$$

where $\Re$ stands for the real part, $\mathbf{E}$ and $\mathbf{H}^{*}$ represent the phasor of the electric field and the complex conjugate magnetic field, respectively. $\mathbf{dA}$ is a vector with amplitude equal to the surface area element dA and direction normal to it; power density (PD) is therefore obtained as P_{dA}/dA.

In close proximity to the human body, part of the stored energy around the antenna might couple into the tissue and human exposure can therefore be affected by the presence of reactive energy. Power density assessed in free-space does not provide a direct measure of this effect. Therefore, in order to evaluate this factor in the targeted frequency range, the field generated by the source, $\mathbf{E}_{\mathrm{inc}}(x,y,z)$, was first represented by a superposition of plane waves, each propagating along a certain direction identified by the couplet $\mathbf{k} = (k_{\mathrm{x}}\hat{\mathbf{x}} + k_{\mathrm{y}}\hat{\mathbf{y}})$, as:

$$\mathrm{E}_{\mathrm{inc}}(x,y,z) = \int\int \hat{\mathrm{E}}_{\mathrm{inc}}(k_{\mathrm{x}},k_{\mathrm{y}},z_0)e^{-i(k_x x+k_y y)}\mathrm{d}k_x\mathrm{d}k_y\cdot e^{-ik_z(z-z_0)} \tag{2}$$

where $\hat{\mathbf{E}}_{\mathrm{inc}}(k_{\mathrm{x}},k_{\mathrm{y}},z)$ corresponds to the complex coefficients of the plane wave spectrum (PWS) on a plane $z = z_0$ given by the Fourier transform of the electric field [21]; $k_z^2 = k^2 - k_x^2 - k_y^2$ where k is wave number in free-space. For $k_x^2 + k_y^2 \le k^2$, the plane waves are propagating while the waves corresponding to $k_x^2 + k_y^2 > k^2$ decay exponentially with increasing z. The evanescent waves characterize the stored energy or the reactive near field.

For each of the waves of the angular spectrum representation impinging on the body surface, $\hat{\mathbf{E}}_{\mathrm{inc}}$, there will be a transmitted plane wave, $\hat{\mathbf{E}}_{\mathrm{tx}}$, so that

$$\hat{\mathbf{E}}_{\mathrm{tx}}(\mathbf{k}) = \mathbf{\Pi}_0(\mathbf{k})\,\hat{\mathbf{E}}_{\mathrm{inc}}(\mathbf{k}), \tag{3}$$

where $\mathbf{\Pi}_0(\mathbf{k})$ is the spectral transmission operator [21] for the planar interface ($z = z_0$) corresponding to the tissue model surface. The PWS of the magnetic field, determined solving Maxwell's equations, is:

$$\hat{\mathbf{H}}_{\mathrm{tx}} = \frac{1}{\omega\mu}\left(k_z\hat{\mathbf{z}} + \mathbf{k}\right)\times\left(\hat{\mathbf{E}}_{\mathrm{tx}}\right), \tag{4}$$

where ω and μ are respectively the angular frequency and the permeability inside the lossy tissue media. The absorbed power within the tissue was therefore determined as:

$$P_{\mathrm{absPWS}} = \frac{1}{2}\int\int\left(\mathbf{E}_{\mathrm{txPWS}}\times\mathbf{H}^{*}_{\mathrm{txPWS}}\right)\cdot\hat{\mathbf{z}}dxdy, \tag{5}$$

where $\mathbf{E}_{\mathrm{txPWS}}$ and $\mathbf{H}_{\mathrm{txPWS}}$ were calculated using expression (2) from $\hat{\mathbf{E}}_{\mathrm{tx}}$ and $\hat{\mathbf{H}}_{\mathrm{tx}}$, respectively. P_{absPWS} determined in this fashion would include both the contribution from the active and reactive incident fields. To evaluate the contribution from the reactive near field, P_{absPWS} was then compared with the absorbed energy due only to the evanescent components of the angular spectrum, $P_{\mathrm{absREACTIVE}}$. The fraction of the total absorbed power originating from the reactive field was studied as a function of the distance to the source and for different antennas and frequencies.

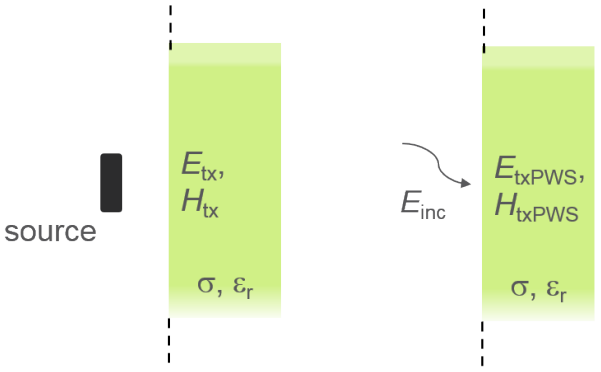

FIGURE 2. Schematic drawing of the applied methodology. On the left, the transmitted fields within the homogenous half-space are determined by means of full-wave simulations, thus including the interactions between the source and the tissue model. On the right, the transmitted fields are obtained by means of the PWS approach using the incident field emitted by the antenna in free-space, $\mathbf{E}_{\mathrm{inc}}$, thereby neglecting the interaction of the source with the tissue model.

B. EFFECT OF MULTIPLE TRANSMISSION ON THE ABSORBED ENERGY

In the analysis above, making use of the PWS, the incident field which is not absorbed at the tissue interface is assumed to be reflected away without interacting with the antenna (zero order interaction). As stated above, however, part of the reflected energy might be scattered by the antenna back towards the body. This iterative process might give raise to several scattering and reception-emission phenomena which might alter the field effectively impinging on the tissue surface. The resulting transmitted and reflected waves might generate a (partial) standing wave, whose effect can be evaluated by comparing the absorbed energy profile when isolating the contribution from the zero-order interaction with the true dissipated energy. The amplitude of $\mathbf{E}_{\mathrm{txPWS}}$ (see Section II.A) was therefore compared with the amplitude of the electric field at the surface inside the skin, $\mathbf{E}_{\mathrm{tx}}$, determined when the full interaction between the source and body model is considered (see Fig. 2). In order to isolate this effect, results in Section III.B are provided assuming perfect matching at the antenna (by scaling the fields to a transmit power of 1 W).

C. ANTENNA MISMATCH

The presence of the body close to the transmitting source might lead to a change in the antenna input impedance. If the device antenna is designed to transmit in free-space, the induced mismatch will cause a reduction in the transmit power. In principle, however, for a poorly matched antenna in free space, this change could lead to a better matching condition when a device is used next to the body. Since com-

pliance with the exposure limits above 10 GHz is assessed in free space, the relevance of this effect was evaluated at the frequencies and for the antenna models described above. The following quantity was determined for each source:

$$\Gamma(d,f) = \left| \frac{Z(d,f) - Z_{\text{freespace}}}{Z(d,f) + Z_{\text{freespace}}} \right| \tag{6}$$

$Z(d,f)$ corresponds to the antenna input impedance as a function of distance to the tissue model surface, d, for the operating frequency f. $Z_{\text{freespace}}$ is the antenna input impedance in free-space; since the antenna dimensions were scaled with the wavelength this quantity is independent of the frequency. Γ would therefore measure the reflection coefficient at the antenna port assuming the antenna is matched in free-space.

$Z(d,f)$ was assessed with FEKO (Altair, Stellenbosch, South Africa) by modelling the skin as the homogenous half-space described in the previous sections.

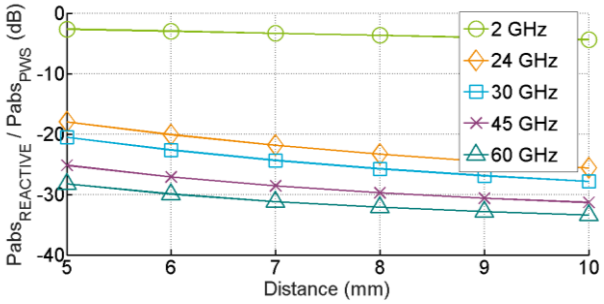

FIGURE 3. Contribution of the reactive near field to the dissipated energy for the dipole array at 24 GHz as a function of the separation distance from the antenna to the homogeneous half-plane.

III. RESULTS

A. EFFECT OF THE REACTIVE NEAR-FIELD

In Fig. 3 the contribution of the reactive near-field, $P_{\text{absREACTIVE}}$, to the total absorbed power determined through the PWS approach, P_{absPWS}, is shown for the 4 elements dipole array as a function of the distance to the lossy media (from 5 mm to 10 mm). At frequencies above 24 GHz and for a separation distance of 5 mm the reactive field contributes to less than 2% of the total dissipated power. As a term of comparison, at 2 GHz the corresponding number would be larger than 50%. The values for the other selected antennas at 24 GHz and above are shown in Table 2 (for separation distances of 5 mm and 10 mm) and are larger than what was obtained for the dipole array. This can be explained by seeing the dipole array as characterized by 8 elements, i.e. by adding four image dipoles which models the effects of the ground plane. The separation distance between the tissue model and the overall radiating structure is therefore larger than what measured from the real physical elements and the contribution from the exponentially decaying evanescent waves is smaller. As expected, the effect of the reactive near field decreases when increasing the frequency and the separation distance to the antenna.

TABLE 2. Contribution of the reactive near field to the total absorbed power in percentage $P_{\text{absREACTIVE}}/P_{\text{absPWS}}*100$.

frequency and separation distance	24GHz		30 GHz		45 GHz		60 GHz	
	5 mm	10 mm	5 mm	10 mm	5 mm	10 mm	5 mm	10 mm
Dipole	9	3	6	2	3	<1	2	<1
PIFA	14	5	10	4	6	2	3	1
Dipole Array	2	<1	<1	<1	<1	<1	<1	<1
Notch Array	10	4	8	3	5	2	3	1

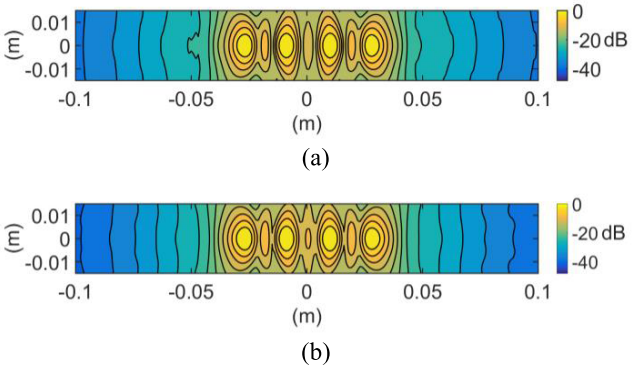

FIGURE 4. Distribution of the absorbed energy at the tissue model surface normalized to the peak value for the notch array at 24 GHz (5 mm separation distance); (a) obtained by means of full-wave simulations; (b) obtained with the plane wave spectrum approach, i.e. neglecting the interaction of the antenna with the tissue model.

Fig.4 (a) and Fig.4 (b) provide a comparison of the energy absorption (normalized to the maximum) on the surface of the tissue model at 5 mm from the notch array, obtained by full-wave simulations, $|\mathbf{E}_{\text{tx}}|^2$, and with the PWS approach, $|\mathbf{E}_{\text{txPWS}}|^2$, at 24 GHz (the squared amplitude of the electric field is proportional to the density of absorbed power). The two plots are almost identical and indicate that, even in close proximity of the tissue model, the profile of the energy distribution is well characterized by the field transmitted by the antenna in free-space. The same observation was made for the dipole array (Fig. 5) and for the other sources.

B. EFFECT OF MULTIPLE TRANSMISSION ON THE ABSORBED ENERGY

The maximum values of $|\mathbf{E}_{\text{tx}}|^2$ and $|\mathbf{E}_{\text{txPWS}}|^2$ at the surface of the tissue model when averaged over 1 cm^2, 4 cm^2 and 20 cm^2 (according to the applicable averaging areas provided today for incident power density by the exposure standards, e.g. [1], or as proposed in [6]) are presented in Fig. 6 for the notch array at 24 GHz as a function of the separation distance. Spatially averaged rather than peak values are presented as these are more relevant to characterize exposure [8]. In this section, the assessments were made for a total transmit power of 1 W by neglecting the possible mismatch at the antenna ports (the effect of antenna mismatch is addressed separately

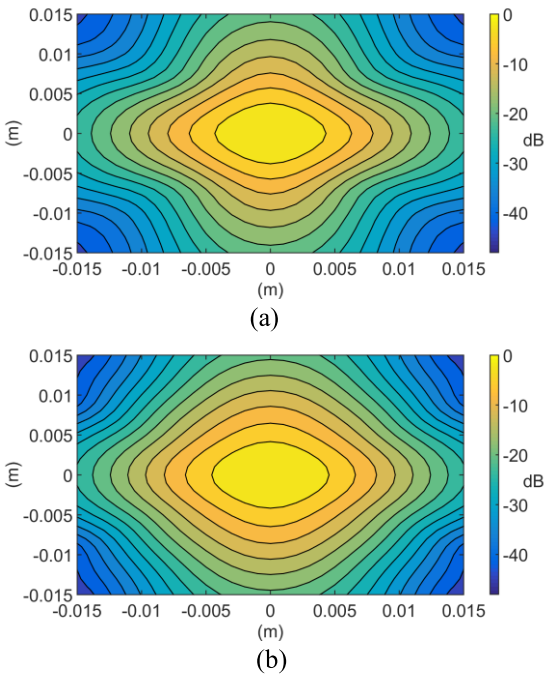

FIGURE 5. Distribution of the absorbed energy at the tissue model surface normalized to the peak value for the dipole array at 24 GHz (5 mm separation distance); (a) obtained by means of full-wave simulations; (b) obtained with the plane wave spectrum approach, i.e. neglecting the interaction of the antenna with the homogeneous skin layer.

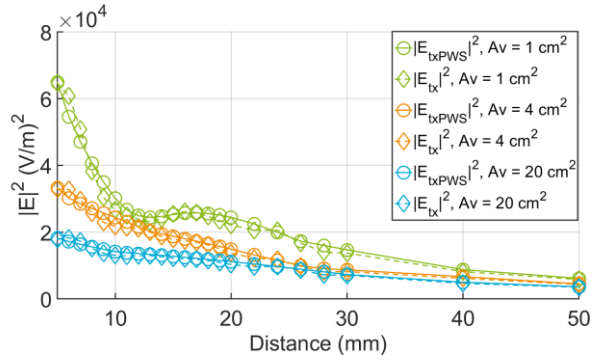

FIGURE 6. Maximum squared amplitude of the spatial-averaged electric field on the tissue model surface for the notch array at 24 GHz and for 1 W transmit power, when determined by means of full-wave simulations, $|\mathbf{E}_{tx}|^2$ compared with the plane wave spectrum approach, $|\mathbf{E}_{txPWS}|^2$ (i.e. neglecting the interaction of the antenna with the tissue model). The results are provided for three different averaging areas, *Av*, 1 cm^2, 4 cm^2 and 20 cm^2 and as a function of the separation distance to the tissue model.

in Section III.C). It is found that for the selected notch array antenna, the effect of the interaction with the tissue model is negligible not only to determine the absorption profile (Fig. 4), but also to characterize the absolute value of the dissipated energy.

In Fig.7 the same comparison was made for all investigated antennas at 24 GHz and for an averaging area of 4 cm^2. As for the notch array, the curves for the dipole and the PIFA almost overlap indicating that the interaction with the tissue

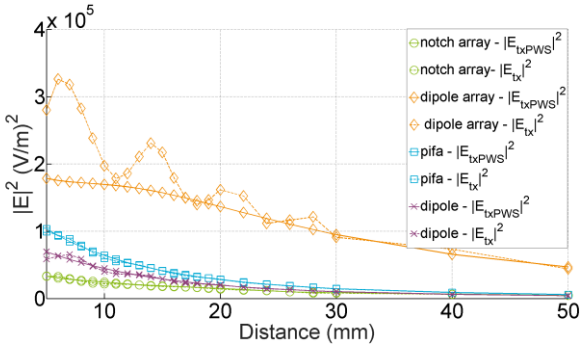

FIGURE 7. Maximum squared amplitude of the electric field on the skin layer averaged over 4 cm^2 for the investigated antennas at 24 GHz and for 1 W transmit power. The values determined by means of full-wave simulations, $|\mathbf{E}_{tx}|^2$ are compared with those obtained using the plane wave spectrum approach, $|\mathbf{E}_{txPWS}|^2$ (i.e. neglecting the interaction of the antenna with the homogeneous tissue model).

model does not lead to any relevant change in the amount of energy absorbed. For the dipole array at 24 GHz and for separation distances less than 30 mm, the effect of multiple reflections between the antenna and the body interface leads instead to an increase of the absorbed energy (although the topography of the energy distribution is not affected, see Fig.4). This is likely because of the relatively large ground plane of the dipole array the energy initially impinging on the tissue model surface is reflected towards the antenna and re-scattered towards the phantom. By progressively increasing the distance a greater part of the transmitted power is reflected away from the antenna structure and this effect becomes less important. The oscillatory behavior is caused by the interference pattern generated by the multiple transmitted and reflected waves. Such arguments are supported by the fact that $|\mathbf{E}_{tx}|^2$ presents a periodic behavior with periods of $\lambda/2$. At this distance, the transverse wave which is reflected at the phantom surface and retransmitted has accumulated during its path a phase shift of 2π. This phenomenon is only visible for the dipole array, which is electrically larger than the other investigated antennas and characterized by a smaller beamwidth. As a consequence, a larger fraction of the energy reflected from the skin interacts with the antenna structure rather than propagate away from it.

C. ANTENNA MISMATCH

The comparisons in Fig.6 and Fig.7 do not consider the possible antenna mismatch due to the presence of the body in close proximity to the antenna as the values are provided for a total output power of 1 W disregarding of the matching condition. The reflection coefficient Γ in (6) is presented in Fig.8 for a distance to the tissue model of 5 mm. For the PIFA, the dipole and the notch array, the presence of the body does not seem to perturb the antenna input impedance; on the contrary for the dipole array, the reflections between the antenna and the homogeneous layer lead to a change in the input impedance as compared when in free-space. The effect

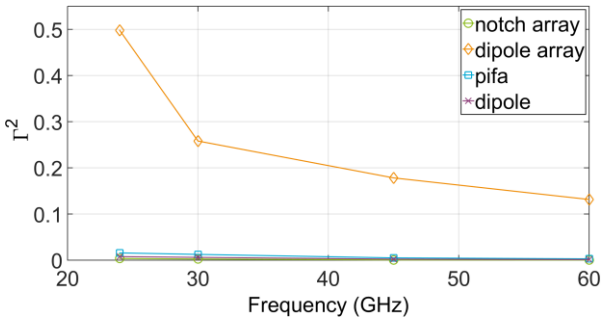

FIGURE 8. Squared value of the reflection coefficient Γ as function of the frequency for a separation distance of 5 mm.

of the mismatch on the absorbed energy is studied in Fig. 9 by scaling $|\mathbf{E}_{\text{tx}}|^2$ with $1 - |\Gamma|^2$. The curves are plotted for the dipole array at different frequencies and as a function of the separation distance. The mismatch at the antenna port tends to scale down $|\mathbf{E}_{\text{tx}}|^2$ reducing the effect of the increased energy absorption due to antenna mismatch.

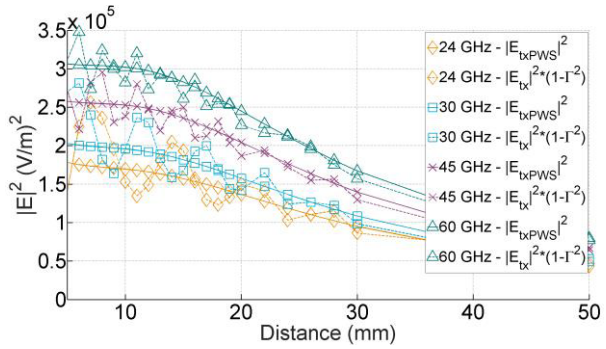

FIGURE 9. Maximum squared amplitude of the electric field at the tissue model surface averaged over 4 cm^2 for the dipole array transmitting 1 W. The values determined by means of full-wave simulations, $|\mathbf{E}_{\text{tx}}|^2$ were scaled with $1 - \Gamma^2$ to include the effect of mismatch at the antenna port and compared with those obtained using the plane wave spectrum approach, $|\mathbf{E}_{\text{txPWS}}|^2$ (i.e. neglecting the interaction of the antenna with the tissue model).

IV. DISCUSSION

Above 24 GHz and for the investigated separation distances equal to or larger than 5 mm (i.e. larger than about 0.4λ), the reactive near field provides a much more modest contribution to power absorption compared with the frequency bands below 6 GHz used today for mobile communication (see Fig.3 and Table 1). According to CENELEC [22], a separation distance of 5 mm or less should be used for compliance assessments of body worn, body supported or garment integrated devices when measuring SAR. In this work, the distance is determined from the antenna which, including the device casing, would translate into a shorter separation from the device. For instance, for devices intended to be used next to the ear, where the antenna is typically placed on the opposite side of the screen, the antenna separation is about as large as the device thickness even when the device is touching the cheek. Therefore, the minimum separation distance selected in this work is consistent with what currently specified by [22]. In any case, as indicated by [8], the contribution from the reactive near field is not expected to be dominant for distances greater than $\lambda/(2\pi) = 2$ mm at 24 GHz.

For the cases investigated the distribution or topographies of the absorbed energy obtained for the antenna transmitting in free-space (i.e. neglecting the possible coupling and interactions of the source with the skin) is almost identical to what obtained with full wave simulations (see Fig. 4 and Fig. 5). This is in line with what was previously found in [23] at the lower frequencies (900 MHz and 1800 MHz) for half-wavelength dipole antennas. Fig. 6 and Fig. 7 indicate also that the free-space electromagnetic field can be used as a good estimate of the absorbed energy (and not only for its distributions) for the dipole, the PIFA and the notch array. For the dipole array it was found that, because of the reflector, the field is transmitted back and forth between the antenna and the lossy media. The energy absorbed is therefore larger than predicted by the zero-order interaction. The difference displays an oscillatory behavior which attenuates with distance and with increased frequency. Because of the multiple interactions, the amount of energy which is reflected and coupled within the port of the dipole array is larger leading to a change in the input impedance whereas for the other antennas the reflection coefficient Γ was substantially zero. When considering the effect of mismatch, the difference in the 'unperturbed' energy absorbed compared with the actual value is reduced. In Fig. 9 the maximum difference between the curves for the dipole array is about 30% at 24 GHz and 10% at 60 GHz. For the other antennas considered $|\mathbf{E}_{\text{tx}}|^2$ and is substantially equal to $|\mathbf{E}_{\text{txPWS}}|^2$. Based on these results, the field of the antenna in free-space seems to characterize quite well the absorbed energy in the tissue in the millimeter wave frequency bands. This is different from the lower frequency case below 10 GHz, where the reactive energy dominates at short distances.

The results of Section III were obtained by assuming that the antennas transmit directly towards the skin tissue modelled as a semi-infinite half space. During typical exposure conditions, however, only a portion of the transmitted energy will impinge on the surface of the body. In particular, to compensate for the large body-shadowing which characterizes these frequencies [23], it is envisioned that portable devices will make use of multiple antenna systems and designs to direct the energy away from the human body during operation. The influence of the body on the antenna transmission is therefore expected to be even smaller than what is presented in this paper.

In this work, the body was modelled as a homogenous half-space of skin tissue which according to [16] can be used as a reasonable approximation when evaluating power absorption in the millimeter wave range. Recent papers have made use of a similar approach e.g. [4], [5], and [7]. The effect of tissue layering on power absorption, could be considered for future

studies. In addition, although wireless devices are foreseen to be used mainly in close proximity of the skin, it could be of interest to investigate the characteristics of energy absorption in more sensitive tissues of other organs such as the eyes.

V. CONCLUSION

Energy absorption mechanisms and near-field body-antenna interactions were studied at frequencies of relevance for the next generation of mobile communication networks, 5G. While at the lower frequencies (e.g. 2 GHz) and for short separation distances, the energy deposition is dominated by the coupling of the reactive near-field, at 24 GHz and above this factor is small and it becomes negligible for device to body separation distances larger than 1 cm.

For the frequency range investigated, the largest increased power absorption, compared with the zero-order interaction, was found for an exposure scenario with significant multiple reflections between the antenna and the body surface: part of the reflected energy at the skin interface interacts with the antenna and is scattered back towards the body. The presence and relevance of this phenomenon is dependent by the antenna design, the separation distance and operating frequency. This effect is expected to be visible only for electrically large antennas and it decreases with increased separation distance and frequency. Despite the multiple reflections, the spatial energy distribution (the topography) was found to be well characterized by the free-space incident field.

The effect of multiple reflections, when present, contributes to a change in the input impedance of the antenna. For an antenna designed for free space conditions, the induced mismatch contributes to a lowering of the output power compared with the free-space condition which, in part, mitigate the effect of enhanced power absorption.

At or around the millimeter wave range, the electromagnetic fields from the antenna in free-space can be used to characterize the energy absorption in the skin also for devices intended to be used in close proximity of the body. In addition, since the contribution from coupling of the reactive near-field is small, free-space power density seems a reasonable quantity to characterize exposure in the 'higher' frequency range of interest for mobile communications (24 GHz to 100 GHz). Overall, in relation to the wide safety margins typically included in the exposure limits, the effects of near-field body interactions are negligible when evaluating compliance at the mmW.

REFERENCES

[1] The International Commission on Non-Ionizing Radiation Protection, "Guidelines for limiting exposure to time-varying electric, magnetic, and electromagnetic fields (up to 300 GHz)," *Health Phys.*, vol. 74, no. 4, pp. 494–522, Apr. 1998.

[2] *Human Exposure to Radio Frequency Fields From Hand-Held and Body-Mounted Wireless Communication Devices—Human Models, Instrumentation, and Procedures—Part 1: Procedure to Determine the Specific Absorption Rate (SAR) for Hand-Held Devices Used in Close Proximity to the Ear (Frequency Range of 300 MHz to 3 GHz)*, document IEC 62209-1, 2005.

[3] E. Dahlman, G. Mildh, S. Parkvall, J. Peisa, J. Sachs, and Y. Selén, "5G radio access," *Ericsson Rev.*, vol. 6, pp. 2–7, 2014.

[4] K. R. Foster, M. C. Ziskin, and Q. Balzano, "Thermal response of human skin to microwave energy: A critical review," *Health Phys.*, vol. 111, no. 6, pp. 528–541, 2016.

[5] K. R. Foster, M. C. Ziskin, and Q. Balzano, "Thermal modeling for the next generation of radiofrequency exposure limits: Commentary," *Health Phys.*, vol. 113, no. 1, pp. 41–53, 2017.

[6] Y. Hashimoto *et al.*, "On the averaging area for incident power density for human exposure limits at frequencies over 6 GHz," *Phys. Med. Biol.*, vol. 62, no. 8, pp. 3124–3138, 2017.

[7] K. R. Foster and D. Colombi, "Thermal response of tissue to RF exposure from canonical dipoles at frequencies for future mobile communication systems," *Electron. Lett.*, vol. 53, no. 5, pp. 360–362, 2017.

[8] E. Carrasco, D. Colombi, K. R. Foster, M. Ziskin, and Q. Balzano, "Exposure assessment of portable wireless devices above 6 GHz," *IEEE Antennas Propag. Mag.*, to be published.

[9] B. Xu *et al.*, "Power density measurements at 15 GHz for RF EMF compliance assessments of 5G user equipment," *IEEE Trans. Antennas Propag.*, vol. 65, no. 12, pp. 6584–6595, Dec. 2017.

[10] L. Alon, S. Gabriel, G. Y. Cho, R. Brown, and C. M. Deniz, "Prospects for millimeter-wave compliance measurement technologies [measurements corner]," *IEEE Antennas Propag. Mag.*, vol. 59, no. 2, pp. 115–125, Apr. 2017.

[11] D. Colombi, B. Thors, and C. Törnevik, "Implications of EMF exposure limits on output power levels for 5G devices above 6 GHz," *IEEE Antennas Wireless Propag. Lett.*, vol. 14, pp. 1247–1249, 2015.

[12] B. Thors, D. Colombi, Z. Ying, T. Bolin, and C. Törnevik, "Exposure to RF EMF from array antennas in 5G mobile communication equipment," *IEEE Access*, vol. 4, pp. 7469–7478, 2016.

[13] T. Wu, T. S. Rappaport, and C. M. Collins, "The human body and millimeter-wave wireless communication systems: Interactions and implications," in *Proc. IEEE Int. Conf. Commun. (ICC)*, Jun. 2015, pp. 2423–2429.

[14] N. Kuster and Q. Balzano, "Energy absorption mechanism by biological bodies in the near field of dipole antennas above 300 MHz," *IEEE Trans. Veh. Technol.*, vol. 41, no. 1, pp. 17–23, Feb. 1992.

[15] N. Chahat, M. Zhadobov, L. Le Coq, S. I. Alekseev, and R. Sauleau, "Characterization of the interactions between a 60-GHz antenna and the human body in an off-body scenario," *IEEE Trans. Antennas Propag.*, vol. 60, no. 12, pp. 5958–5965, Dec. 2012.

[16] S. I. Alekseev, A. A. Radzievsky, M. K. Logani, and M. C. Ziskin, "Millimeter wave dosimetry of human skin," *Bioelecromagnetics*, vol. 29, no. 1, pp. 65–70, 2008.

[17] Q. Balzano, M. Y. Kanda, and C. C. Davis, "Specific absorption rates in a flat phantom in the near-field of dipole antennas," *IEEE Trans. Electromagn. Compat.*, vol. 48, no. 3, pp. 563–568, Aug. 2006.

[18] *Studies on Frequency-Related Matters for International Mobile Telecommunications Identification Including Possible Additional Allocations to the Mobile Services on a Primary Basis in Portion(s) of the Frequency Range Between 24.25 and 86 GHz for the Future Development of International Mobile Telecommunications for 2020 and Beyond*, document RESOLUTION 238 (WRC-15), ITU World Radiocommunication Conference, 2015.

[19] W. Roh *et al.*, "Millimeter-wave beamforming as an enabling technology for 5G cellular communications: Theoretical feasibility and prototype results," *IEEE Commun. Mag.*, vol. 52, no. 2, pp. 106–113, Feb. 2014.

[20] S. Gabriel, R. W. Lau, and C. Gabriel, "The dielectric properties of biological tissues: III. Parametric models for the dielectric spectrum of tissues," *Phys. Med. Biol.*, vol. 41, no. 11, pp. 2271–2293, 1996.

[21] C. Scott, *The Spectral Domain Method in Electromagnetics*. Norwood, MA, USA: Artech House, 1989.

[22] *Product Standard to Demonstrate the Compliance of Wireless Communication Devices With the Basic Restrictions and Exposure Limit Values Related to Human Exposure to Electromagnetic Fields in the Frequency Range From 30 MHz to 6 GHz: Hand-Held and Body Moun*, document BS EN 50566:2017, CENELEC, 2017.

[23] B. Derat, A. Cozza, and J.-C. Bolomey, "Influence of source—Phantom multiple interactions on the field transmitted in a flat phantom," in *Proc. EMC Zurich*, Munich, Germany, 2007, pp. 139–142.

[24] K. Zhao, J. Helander, D. Sjöberg, S. He, T. Bolin, and Z. Ying, "User body effect on phased array in user equipment for the 5G mmWave communication system," *IEEE Antennas Wireless Propag. Lett.*, vol. 16, pp. 864–867, 2016.

DAVIDE COLOMBI received the M.Sc. degree (*summa cum laude*) in telecommunication engineering from the Politecnico di Milano, Italy, in 2009. Since 2009, he has been with Ericsson Research, Stockholm, Sweden, where he has been involved in research and standardization related to radio frequency exposure from wireless communication equipment. Since 2014 he has been involved in activities related to EMF compliance of 5G wireless equipment. He is currently a Convener of IEC TC106 AHG 10 and the Deputy Chair of the EMF Standardization Working Group within the Mobile and Wireless Forum.

BJÖRN THORS received the M.Sc. degree in engineering physics from Uppsala University, Sweden, in 1996 and the Ph.D. degree in electromagnetic theory from the Royal Institute of Technology (KTH), Stockholm, Sweden, in 2003. From 2003 to 2005, he was a Research Associate at KTH. Since 2005, he has been with Ericsson Research, where he is currently a Senior Specialist, involved in research and standardization related to radio frequency exposure assessment of wireless equipment.

CHRISTER TÖRNEVIK (M'98) received the M.Sc. degree in applied physics from Linköping University, Linköping, Sweden, in 1986 and the Lic. (Tech.) degree in materials science from the Royal Institute of Technology, Stockholm, Sweden, in 1991. He joined Ericsson in 1991, and has, since 1993, been involved in research activities related to radio frequency exposure from wireless communication equipment. He is currently a Senior Expert with Ericsson Research and is responsible for electromagnetic fields and health within the Ericsson Group. From 2003 to 2005, he was the Chairman of the Board of the Mobile Manufacturers Forum, and he is currently the Secretary of the Board. Since 2006, he has been the Chairman of the Technical Committee on Electromagnetic Fields within the Swedish Electrotechnical Standardization Organization, SEK, and he has as an Expert contributed to the development of several CENELEC, IEC, and IEEE standards on the assessment of RF exposure from wireless equipment.

QUIRINO BALZANO received the Doctorate degree in electronics engineering from the University of Rome, Rome, Italy, in 1965. During 1966, he was at FIAT, SpA, Turin, Italy. From 1967 to 1974, he was with the Missile Systems Division, Raytheon Company, Bedford, MA, USA. He was involved in the research, design, and development of planar and conformal phased arrays for the Patriot and other missile systems. In 1974, he joined Motorola, Inc. Portable Products Division, Plantation, FL, USA, where he achieved the position of Corporate Vice President and the Director of Portable Products Research Laboratories. His group was essential in the development of the cell phone technology. He retired from Motorola in 2001. Since 2002, he has been at the Department of Electrical and Computer Engineering, University of Maryland, College Park, MD, USA, where he is a Senior Staff Researcher. He teaches courses on antennas at American, European, and Asian universities. His main interest is in antennas, the biological effects of human exposure to RF electromagnetic energy, and electromagnetic interference with medical devices. He has authored over 50 papers on antennas, RF dosimetry near electromagnetic sources and the biological effects of RF energy. He has 31 patents in antenna and IC technology and has authored or co-authored over 120 papers and publications.